Adaptive Gabor filters for phase-based disparity estimation

Bruno Crespi
ITC – IRST
I-38050 Povo, Trento, Italy
e-mail:crespi@irst.itc.it

Abstract

The phase-difference-based technique has become a widespread method for depth and optical flow estimation because of superior performance and better theoretical groundings. The technique is based on the convolution of the stereo image pair with Gabor filters. Gabor filters contains two parameters, the width and the tuning frequency. In order to optimize performance, these parameters have to be chosen in accordance to the characteristics of the visual signal. In this article we propose an automatic technique to locally adapt the filter parameters to the input signal. In the first part, we analyze the performance of the phase-difference-based technique for disparity estimation with respect to the choice of the Gabor filter parameters. In particular we characterize the effects of phase nonlinearities on the quality of disparity estimates. In the second part, a novel technique is introduced that reduces phase nonlinearity by means of an adaptive mechanism for the tuning frequency. The performance improvement produced by the adaptive filter is demonstrated on computer simulated and random-dot stereo images. Results show the proposed technique allows a substantial improvement of disparity estimation.

Keywords: Stereo vision, Phase-based technique, Adaptive Gabor filters.

1 Introduction

Disparity estimations are based on the simplified assumption that the stereo signals, $f^R(x)$ and $f^L(x)$, are *locally* related by a one-dimensional shift, the disparity $d(x)$, along the epipolar lines,

$$f^L(x + d(x)/2) = f(x) = f^R(x - d(x)/2) \quad (1)$$

Various methods have been devised to measure the disparity of corresponding points. While the "correspondence" method [1, 7] is based on the search of corresponding points, the phase-difference-based technique, developed by [8], relies on the computation of the phase difference between the convolutions of the two stereo images with Gabor filters. This technique is based on the observation that assumption (1) implies that in the neighborhood of each point x_0 the local k-frequency components, $\phi_k^{L/R}(x_0)$, of signals $f^{L/R}(x)$ are related by phase difference $\Delta\phi(x_0) = \phi_k^L(x_0) - \phi_k^R(x_0) = k\, d(x_0)$. This local spectral analysis is performed by convolving the images with a local envelope tuned at the desired peak tuning frequency, $\nu_0 = k_0/2\pi$,

$$\begin{aligned} u^{L/R}(x, k_0) &= \int dy\, G(x-y)\, e^{i\, k_0 (x-y)}\, f^{L/R}(y) \\ &= \rho^{L/R}(x)\, e^{i\, \psi^{L/R}(x)} \end{aligned} \quad (2)$$

where

$$G(x) = \frac{1}{\sqrt{2\,\pi}\,\sigma}\, e^{-\frac{(x-x_0)^2}{2\sigma^2}} \quad (3)$$

Convolutions $u^{L/R}(x, k_0)$ measure the k_0 frequency content of the stereo signals in a small neighborhood of position x[1].

The Gabor filter, $G(x)\, e^{i\, k_0 (x)}$, is characterized by two parameters: σ measures the width of the local envelope and k_0 the tuning frequency. The relative magnitude of the two parameters determines how many oscillations of wavelength $\lambda = 1/\nu_0$ take place inside a region in which the filter is significantly different from zero. For example, the choice of one-octave Gabor filters, $\sigma\, k_0 = 3$, means that there is one oscillation in the region $[x_0 - \sigma,\, x_0 + \sigma]$, i.e. $\lambda = 2\pi/k_0 \approx 2\,\sigma$.

The phase, $\psi(x) = \mathrm{Im}[\log u(x)] \in [-\pi,\, \pi]$, is selected as the function from which the shift is computed because of its "quasi-linear" behavior [5]. In

[1] In the following indexes L/R are sometimes dropped for notation simplicity.

fact, phase derivative $\psi_x(x)$ is generally close to the value of the tuning frequency $\psi_x(x) \approx k_0$. Linearity allows an accurate estimation of the shift from the phase difference by means of a second order expansion in $d(x)$, [2]

$$\begin{aligned} \Delta\psi(x) &= \psi^L(x) - \psi^R(x) \\ &= \psi(x - d(x)/2) - \psi(x + d(x)/2) \\ &= \psi_x(x)\, d(x) + O(d^3(x)). \end{aligned} \quad (4)$$

where $\psi^L(x+d(x)/2) = \psi(x) = \psi^R(x-d(x)/2)$. Using the average of the derivatives, disparity is given by

$$d(x) \approx 2\, \frac{[\Delta\psi(x)]_{2\pi}}{\psi_x^L(x) + \psi_x^R(x)}. \quad (5)$$

The phase is a quasi-linear function except near points of vanishing amplitude, $\rho(x) = 0$, where it may present a strong non-linear behavior. Around these singular points disparity calculation fails [4, 5]. Computation is considered reliable wherever the following inequality holds

$$|\, \psi_x(x) - k_0 \,| \;<\; k_0\, T_S \quad (6)$$

where $T_S \approx 0.4$.

This quantity is an indication of phase linearity. In fact the left side of (6) measures the difference between the peak frequency, k_0, and the local frequency, $\psi_x(x)$. Larger values of threshold T_S may increase the density of "reliable points" but determines a sharp increase of the error on disparity estimates [3]. To increase density without increasing error, banks of filters of increasing widths and wavelengths may be employed and their responses combined [6].

2 Performance of the Gabor filters

The choice of the filter parameters, σ and k_0, is dictated by several qualitative considerations. The wavelength $\lambda = 1/\nu_0 = 2\pi/k_0$, has to be at least twice as large as the expected maximum disparity to avoid wraparound effects [3]. The filter support, i.e. the region in which the filter is significantly different from zero, should be larger than the expected maximum disparity, so that the left and right convolutions comprise the same visual features.

Furthermore, since phase "linearity" is the principal requirement for a reliable disparity estimation, for a given stereo signal filter parameters should be adjusted in order to produce a response as linear as possible.

For well-defined stereo signals (for example isolated spikes) the phase is a quasi-piecewise linear function $\psi_x(x) \approx k_0$. Transitions between quasi-linear regions occur where the amplitude is small, i.e. near singular points. Transition steepness is proportional to the width of the Gaussian envelope, σ, see Figures 1 and 2.

2.1 Choice of the filter's parameters

To obtain a significant and quantitative evaluation of the effects of parameters values on disparity estimates, performance was evaluated for a large number of random-dots 1-D images for different values of width and tuning frequency. Performance is measured in terms of error and density of reliable points. The error measure is defined as the absolute difference between the true disparity and the value estimated by the algorithm. Density is the ratio between the number of points where disparity computation is accepted – according to eq. (6) – and the total number of points. The random-dot 1-D images used in the following simulations have zero mean, i.e. $\int f(x)\, dx = 0$.

In the first experiment constant disparity fields are used, i.e. the left image is obtained by a constant shift of the right one. This means that there are no occlusions. Simulations show that performance is optimized if wavelength and filter width are changed concomitantly, i.e. by keeping fixed the ratio between wavelength and width, i.e. $\sigma_n = \lambda_n/2$, $n = 1, 2, 3$, see Figures 3 and 4. The error is almost flat for disparity in the range $[0, \frac{\lambda_n}{3}]$, then it grows rapidly. The density is almost constant.

The value of the ratio between wavelength and width, that measures the number of oscillations within the filter support, is still a free parameter. We notice that within the filter support there should be enough oscillations to allow local frequency estimation, in general the smoothness of the phase function improves by increasing the width for fixed frequency. On the other hand, large filter can cause a loss of resolution and a consequent error increase because the disparities of close-by small visual features are averaged over. A good compromise is the choice $\sigma \approx \lambda/2$.

Once the ratio between width and wavelength is chosen the filter's performance becomes a one parameter function (e.g. the tuning frequency). As a function of the wavelength the typical performance of a Gabor filter estimator is shown in Fig. 5. Inputs are random-dot stereo pairs in which disparity

[2] The second order term is zero, $\psi_{xx}/2!\,(\delta^2(x) - \delta^2(x))/4 = 0$.

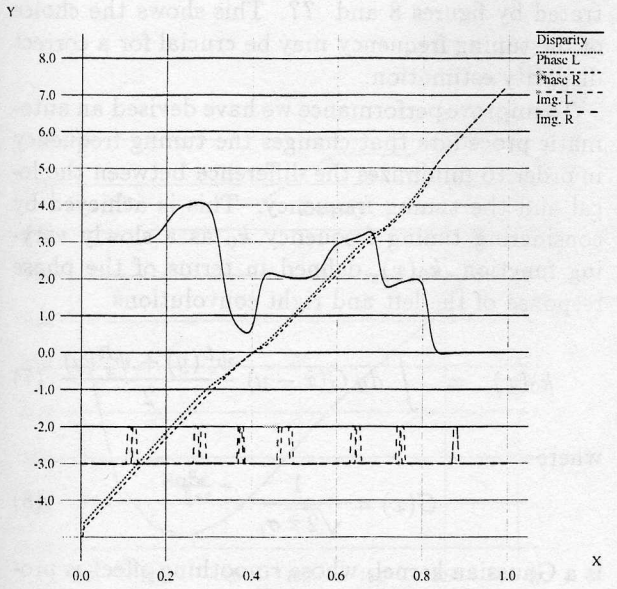

Figure 1: *Showing the left and right phases, $\psi^{L/R}(x)$ for a spike-like 1-D stereo signal composed of $N = 256$ points. Graphs are translated on the y-axis for visualization purposes.*

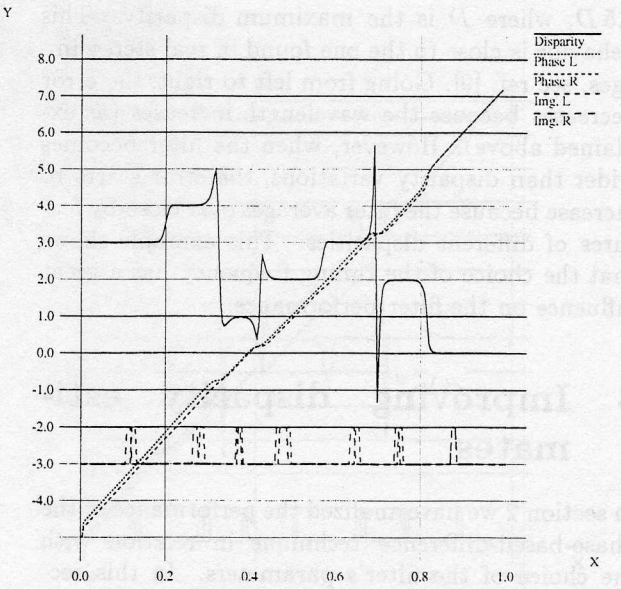

Figure 2: *Narrower filters, for example $\lambda = 20$, $\sigma = 8$, determine sharper transitions between different disparity values but can cause irregularities.*

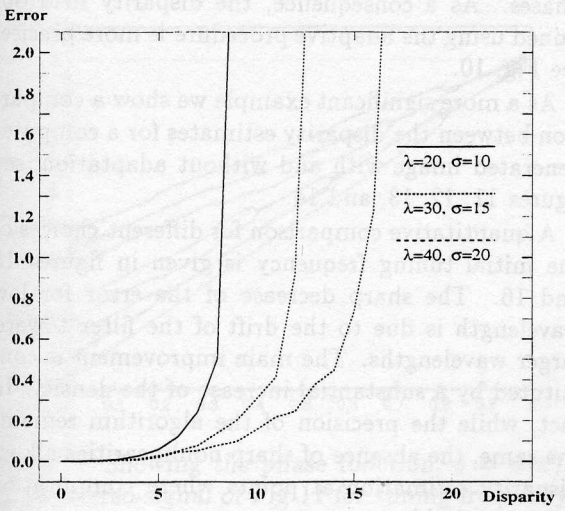

Figure 3: *Errors of disparity estimates for $\lambda_1 = 20$, $\lambda_2 = 30$, $\lambda_3 = 40$ and $\sigma_n = \lambda_n/2$, $n = 1, 2, 3$ for 1-D images of size $N = 512$ pixels.*

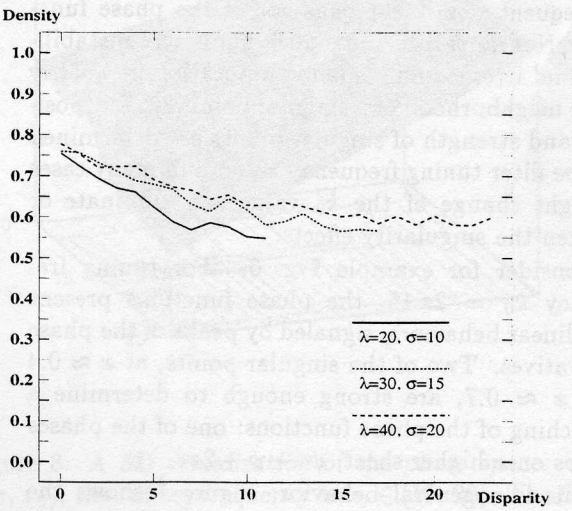

Figure 4: *Densities of disparity estimates.*

assumes random values in the range $[0, D = 5]$ in 20 randomly generated intervals, i.e. disparity is a piecewise constant function.

The error curve displays a minimum for $\lambda_0 \approx 2.5\,D$, where D is the maximum disparity. This behavior is close to the one found in real stereo images, see ref. [9]. Going from left to right, the error decreases because the wavelength increases (as explained above). However, when the filter becomes wider than disparity variations, the error starts to increase because the filter averages over close-by features of different disparities. This example shows that the choice of the tuning frequency has a great influence on the filter performance.

3 Improving disparity estimates

In section 2 we have analized the performance of the phase-based-difference technique in relation with the choice of the filter's parameters. In this section we illustrate how disparity estimates can be improved by adaptating the tuning frequency to the input signal.

3.1 Parameter optimization

The reliability of disparity computation at a given point x is indicated by the local frequency being close to the tuning frequency, see eq. (6). A large discrepancy between local and tuning frequency indicates the presence of a singular points and a consequent non-linear behavior of the phase function. Non-linearities introduce numerical instabilities and irremediably spoil computation in a fairly large neighborhood of a singular point [2]. The position and strength of singular points are determined by the filter tuning frequency k_0, and in many cases a slight change of the k_0 value can eliminate or weaken the singularity effects.

Consider for example Fig. 6. For tuning frequency $k_0 = 2\pi\,15$, the phase functions present non-linear behaviors, signaled by peaks of the phase derivatives. Two of the singular points, at $x \approx 0.4$ and $x \approx 0.7$, are strong enough to determine a branching of the phase functions: one of the phases jumps on a higher sheet, $\psi \rightarrow \psi + 2\pi$.

This is a general behavior; Figure 7 shows the possible phase behaviors for the tuning frequency ν_0 in the range $[10, 20]$. Near singular points, i.e. in the nonlinear regions, phases corresponding to similar signals may become very different.

Therefore, even for simple signals, a correct choice of the tuning frequency is made difficult by a non-trivial structure of the phase space (x, λ). However, a slight change of the tuning frequency value can lead the phase into a more regular region, as illustrated by figures 8 and ??. This shows the choice of the tuning frequency may be crucial for a correct disparity estimation.

To improve performance we have devised an automatic procedure that changes the tuning frequency in order to minimizes the difference between the local and the tuning frequency. This is achieved by considering tuning frequency k_0 as a slowly varying function, $k_0(x)$, defined in terms of the phase response of the left and right convolutions

$$k_0(x) \;=\; \int dy\; G(x-y)\;\frac{\psi_x^L(y) + \psi_x^R(y)}{2} \qquad (7)$$

where

$$G(x) = \frac{1}{\sqrt{2\,\pi}\,\sigma_\nu}\; e^{-\frac{x^2}{2\sigma_\nu^2}} \qquad (8)$$

is a Gaussian kernel, whose smoothing effect is proportional to σ_ν. Convolutions (2) and (7) are successively applied until function $k_0(x)$ becomes stationary.

How adaptation works is shown by Figures 6 and 9. The input signals and the initial filter parameters are the same, however Fig. 9 is produced using the adaptive procedure. Operation 7 changes the value of $k_0(x) = 2\pi\,\nu_0(x)$ in order to minimize the difference between local and tuning frequency. This result is a smoothly varying function $\nu_0(x) \in [11, 13.6]$, which produces quasi-linear phases. As a consequence, the disparity field obtained using the adaptive procedure is more precise, see Fig. 10.

As a more significant example we show a comparison between the disparity estimates for a computer generated image with and without adaptation, see figures 11, 12, 13, and 14.

A quantitative comparison for different choices of the initial tuning frequency is given in figures 15 and 16. The sharp decrease of the error for low wavelength is due to the drift of the filter toward larger wavelengths. The main improvement is constituted by a substantial increase of the density. In fact, while the precision of the algorithm remains the same, the absence of sharp nonlinearities allows disparity estimation at points where computation was not reliable.

Similar improvements are obtained for random-dot 1-D images. Figures 17 and 18 show error and density with and without adaptation for a large number (256) of random-dot images with piecewise

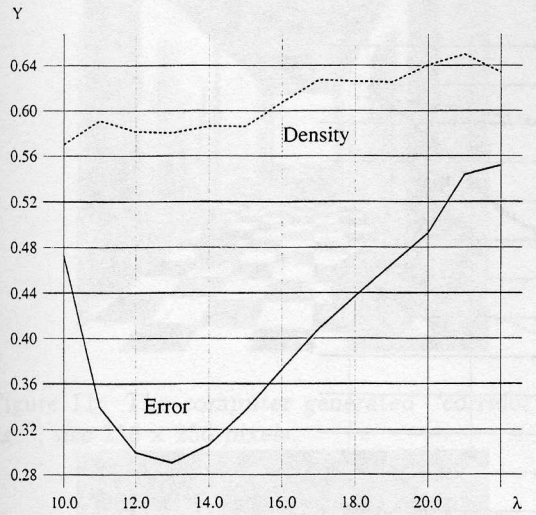

Figure 5: *Piecewise constant disparity field. Error and density for the three filters as a function of the wavelength, with* $\sigma = \lambda/2$ *and* $N = 256$ *. In each stereo pair, disparity assumes random values in the range of* $[0, 5]$ *pixels, in 20 randomly generated intervals. Each point represents the average error or the density on a large number (256) of random-dot 1-D image pairs.*

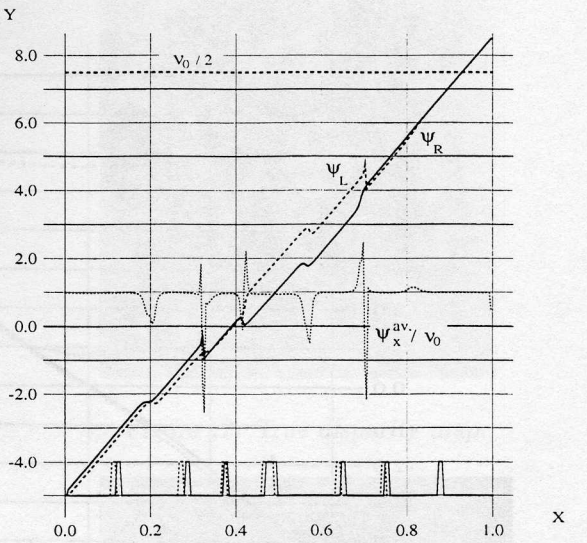

Figure 6: *Showing the phase functions,* $\psi^{L/R}(x)$*, for* $\nu_0 = 15$*,* $\sigma = 13$*, and* $N = 256$*. The irregular behaviors of the phases is clearly illustrated by the sharp peaks in the averaged phase derivative,* $\psi^{av.} = (\psi_x^L + \psi_x^R)/2$*. At the bottom, the left and right signals are shown.*

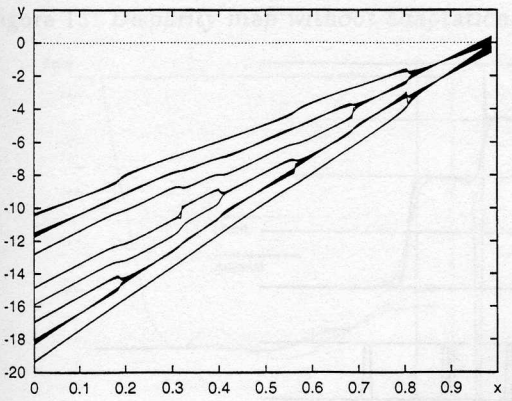

Figure 7: *Showing the phase function,* $y = \psi(x)$*, for the stereo-signal of Fig 11 for tuning frequency* $\psi(x, \nu_0)$*, the tuning frequency is* ν_0 *varying in the range* $[10, 20]$*. The filter width is constant,* $\sigma = 13$*.*

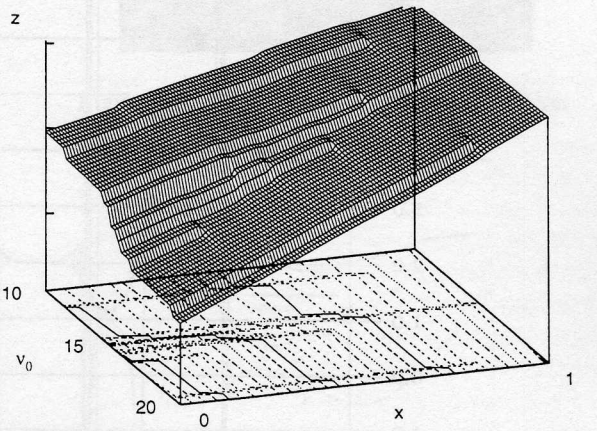

Figure 8: *A 3D visualization of the phase space:* $z = \psi(x, \nu_0)$*, the tuning frequency is* $\nu_0 \in [10, 20]$*. The filter width is constant,* $\sigma = 13$*.*

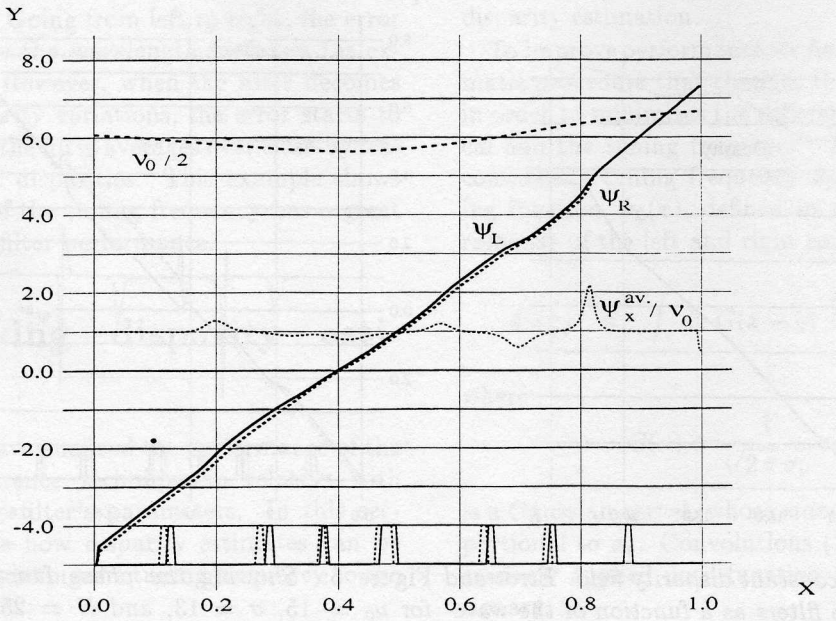

Figure 9: *Showing the phase functions obtained using optimization of the tuning frequency. The initial value* $\nu_0 = 15$ *has changed to* $\nu_0(x) \in [11, 13.6]$. *Now phases have a smoother behavior.*

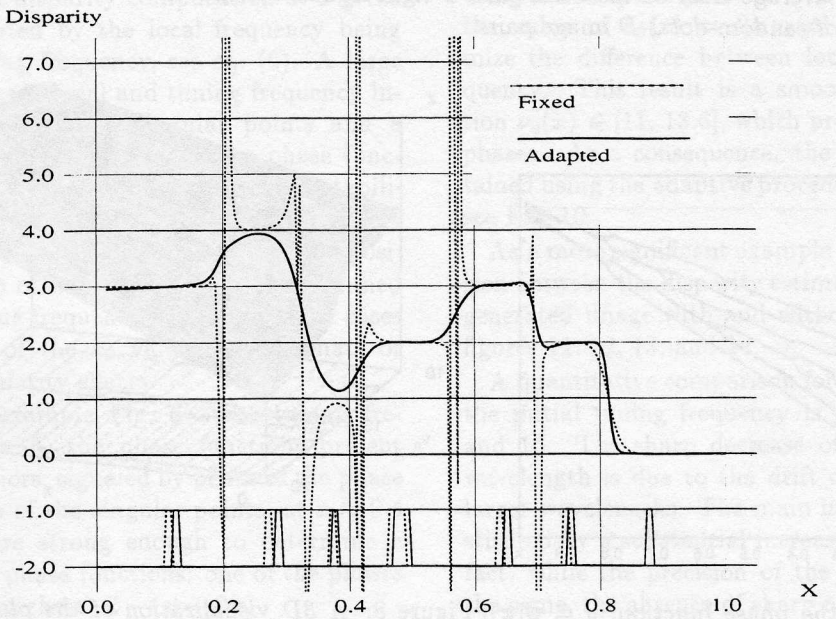

Figure 10: *Comparison between the disparity fields (units are pixels) without and with adaptation of the tuning frequency, corresponding to Fig. 11 and Fig. 15, respectively.*

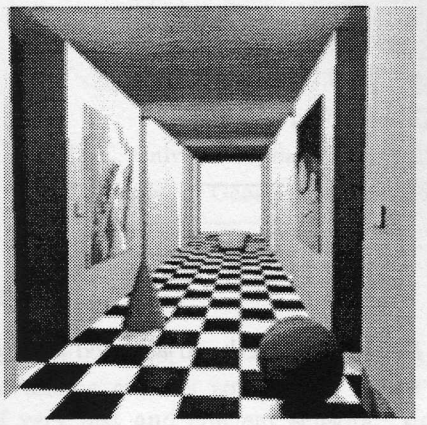

Figure 11: *The computer generated "corridor image", size* 256×256 *pixels.*

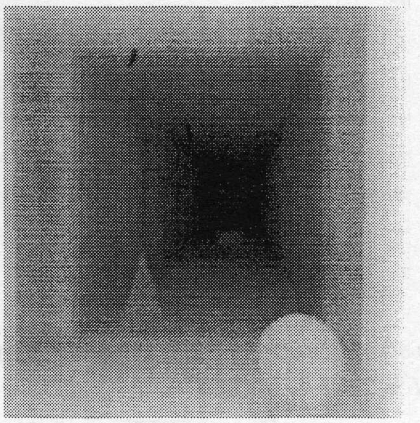

Figure 12: *True disparity map.*

Figure 13: *Disparity map without adaptation.*

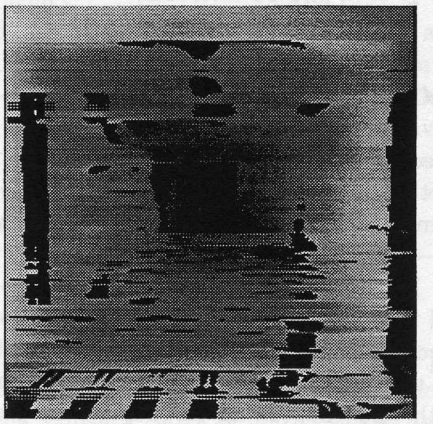

Figure 14: *Disparity map with adaptation.*

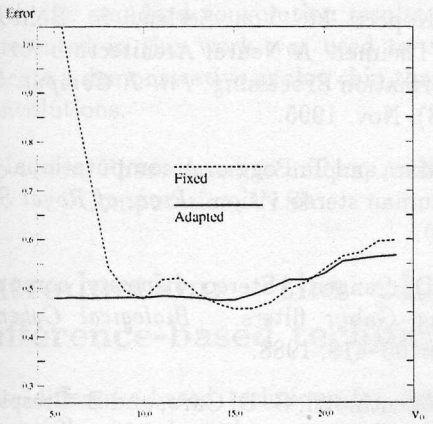

Figure 15: *Error for fixed and adapted tuning frequency for the* 128×128 *corridor image.*

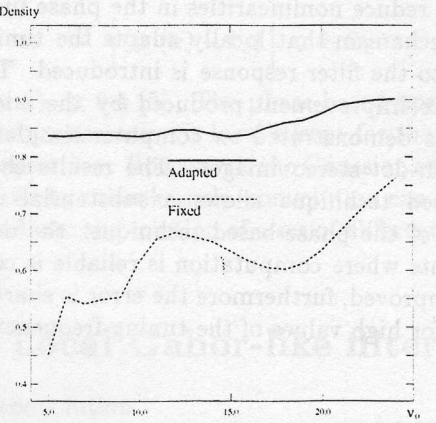

Figure 16: *Density for fixed and adapted tuning frequency for the* 128×128 *corridor image.*

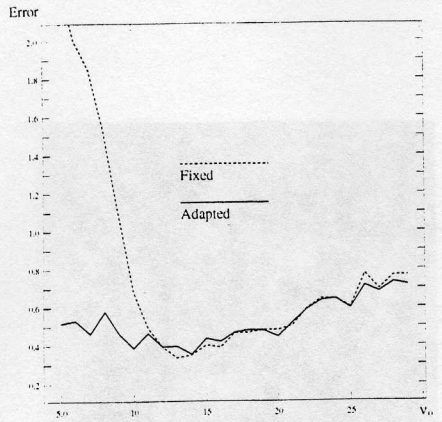

Figure 17: *Error for fixed and adapted tuning frequency, $N = 256$.*

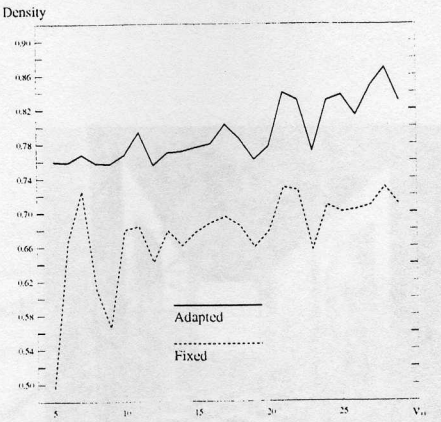

Figure 18: *Density for fixed and adapted tuning frequency, $N = 256$.*

constant disparity fields ($N = 256$ pixels, maximum disparity $D = 5$, and 15 intervals).

4 Conclusions

The objective of this work was to devise a procedure for the automatic adaptation of the Gabor filter parameters – used in phase-based disparity estimation — to the visual characteristics of the input images. In the first part of this article, we have analyzed the performance of the phase-difference-based technique for disparity estimation with respect to the choice of the Gabor filter parameters: the width and the tuning frequency. In particular we have evidenced the close relation between phase linearity and quality of disparity estimations. In order to reduce nonlinearities in the phase functions, a mechanism that locally adapts the tuning frequency to the filter response is introduced. The performance improvement produced by the adaptive filter is demonstrated on computer simulated and random-dot stereo images. The results show the proposed technique allows a substantial improvement of the phase-based technique: the density of points where computation is reliable is consistently improved, furthermore the error is sharply decreased for high values of the tuning frequency.

References

[1] S.T. Barnard and W.B. Thompson. Disparity analysis of images. *IEEE Trans. on Pattern Analysis and Machine Intelligence*, PAMI(2):333–340, 1980.

[2] Cai and Mayhew. A note on some phase differencing algorithms for disparity estimation. *International Journal of Computer Vision*, 22(2):111–124, 1997.

[3] A. Cozzi, B. Crespi, F. Valentinotti, and F. Woergoetter. Performance of phase-based algorithms. *Machine Vision and Application, special issue on Performance Characteristics of Vision Algorithms*, 9(5-6):334–340, 1997.

[4] D. J. Fleet, A. D. Jepson, and M. Jenkin. Phase–based Disparity Measurement. *CVGIP: Image Understanding*, 53(2):198–210, March 1991.

[5] D.J. Fleet and A.D. Jepson. Stability of phase information. *IEEE Transaction on Pattern Analysis and Machine Intelligence*, 1993.

[6] J. Kopecz M. Von Seelen, S. Bohrer and W. Theimer. A Neural Architecture for Visual Information Processing. *Int. J. Comput. Vision*, 16(3), Nov. 1995.

[7] D. Marr and T. Poggio. A computational theory of human stereo vision. *Proc. of Royal Society*, 1979.

[8] T. D. Sanger. Stereo disparity computation using Gabor filters. *Biological Cybernetics*, (59):405–418, 1988.

[9] F. Valentinotti, G. Di Caro, and B. Crespi. Real-time parallel computation of disparity and optical flow using phase difference. *Machine Vision and Applications*, 9(3):87–96, 1996.